PCP
PLANT & CELL PHYSIOLOGY

Rapid Paper

Closing Plant Stomata Requires a Homolog of an Aluminum-Activated Malate Transporter

Takayuki Sasaki[1,5,*], Izumi C. Mori[1,5], Takuya Furuichi[1,5], Shintaro Munemasa[2], Kiminori Toyooka[3], Ken Matsuoka[4], Yoshiyuki Murata[2] and Yoko Yamamoto[1]

[1]Research Institute for Bioresources, Okayama University, Chuo 2-20-1, Kurashiki, Okayama, 710-0046 Japan
[2]Graduate School of Natural Science and Technology, Okayama University, Tsushima-Naka, Okayama, 700-8530 Japan
[3]RIKEN Plant Science Center, Tsurumi-ku, Yokohama, 230-0045 Japan
[4]Laboratory of Plant Nutrition, Faculty of Agriculture, Kyushu University, Higashi-ku, Fukuoka, 812-8581 Japan
[5]These authors contributed equally to this work
*Corresponding author: E-mail, tsasaki@rib.okayama-u.ac.jp; Fax, +81-86-434-1236
(Received January 18, 2010; Accepted February 9, 2010)

Plant stomata limit both carbon dioxide uptake and water loss; hence, stomatal aperture is carefully set as the environment fluctuates. Aperture area is known to be regulated in part by ion transport, but few of the transporters have been characterized. Here we report that *AtALMT12* (At4g17970), a homolog of the aluminum-activated malate transporter (ALMT) of wheat, is expressed in guard cells of *Arabidopsis thaliana*. Loss-of-function mutations in *AtALMT12* impair stomatal closure induced by ABA, calcium and darkness, but do not abolish either the rapidly activated or the slowly activated anion currents previously identified as being important for stomatal closure. Expressed in *Xenopus* oocytes, AtALMT12 facilitates chloride and nitrate currents, but not those of organic solutes. Therefore, we conclude that AtALMT12 is a novel class of anion transporter involved in stomatal closure.

Keywords: ALMT family protein • Anion transporter • AtALMT12 • Stomatal closure.

Abbreviations: ALMT, aluminum-activated malate transporter; CaMV, cauliflower mosaic virus; CBP, calmodulin-binding family protein; GFP, green fluorescent protein; GUS, β-glucuronidase; mRFP, monomeric red fluorescent protein; ORF, open reading frame; OST1, open stomata 1; RT–PCR, reverse transcription–PCR; SLAC1, SLOW ANION CHANNEL-ASSOCIATED 1.

Introduction

Stomatal movement is driven by turgor pressure changes in guard cells, changes predominantly achieved by solute transport through multiple ion channels (Ward et al. 2009). Several of the relevant cation channels, such as for calcium and potassium, have been reasonably well studied (Pilot et al. 2001, Hosy et al. 2003); however, much less is known about the anion channels.

To date, four types of anion channels or transporters have been implicated in stomatal movements. First, an ABC-class transporter, AtABCB14, was identified as a malate importer, modulating stomatal movement by increasing osmotic pressure in guard cells (Lee et al. 2008). Secondly, a nitrate transporter, AtNRT1.1/CHL1, functions in stomatal opening in the presence of nitrate (Guo et al. 2003). The third and fourth type of anion channel activity mediate the rapidly activated (R-type) and the slowly activated (S-type) anion currents, which are implicated in being involved in stomatal closure (Hedrich et al. 1990, Schroeder and Keller 1992, Schmidt et al. 1995, Pei et al. 1997).

Although genes encoding R-type anion currents have yet to be identified, S-type anion currents have recently been discovered to require a gene named *SLOW ANION CHANNEL-ASSOCIATED 1* (*SLAC1*; At1g12480; Negi et al. 2008, Saji et al. 2008, Vahisalu et al. 2008). This gene was isolated in screens for mutants insensitive to carbon dioxide or hypersensitive to ozone, and appears to be a distant homolog of bacterial and fungal dicarboxylate transporters. SLAC1 is localized at the plasma membrane and is essential for stomatal closure in response to carbon dioxide, ABA and ozone (Negi et al. 2008, Vahisalu et al. 2008). However, it is not known whether additional types of anion currents must flow for stomatal aperture control.

Anion channels have also been characterized in connection with aluminum toxicity, which is a major limiting factor of plant growth in acidic soils, because an important resistance pathway involves the secretion of organic anions that chelate aluminum, such as citrate or malate (Ma et al. 2001, Kochian et al. 2004, Delhaize et al. 2007). Indeed, *Triticum aestivum* (wheat) has an aluminum-activated malate-permeable channel, *ALMT1* (also known as *TaALMT1*), that is localized to the plasma membrane, and confers resistance to aluminum (Sasaki et al. 2004, Yamaguchi et al. 2005, Zhang et al. 2008). Genes with apparent homology to *TaALMT1* are plant specific. Among 13

Plant Cell Physiol. 51(3): 354–365 (2010) doi:10.1093/pcp/pcq016, available online at www.pcp.oxfordjournals.org

Arabidopsis thaliana genes similar to *TaALMT1*, *AtALMT1* is likewise an aluminum-activated malate transporter, expressed in roots and related to aluminum resistance (Hoekenga et al. 2006). In contrast, *AtALMT9* encodes a vacuolar malate channel, unrelated to aluminum but apparently involved in malate homeostasis, and is mainly expressed in leaf mesophyll (Kovermann et al. 2007). Also independent of aluminum resistance, a maize homolog, *ZmALMT1*, transports little if any malate and instead transports inorganic anions (Piñeros et al. 2008b). Therefore, ALMT-type anion channels have multiple functions in anion homeostasis, contributing to the regulation of growth and response to the environment.

Here, we show that AtALMT12 is an anion transporter, particularly permeable to chloride and nitrate, and a key regulator of stomatal closure.

Results

The role of AtALMT12 in stomatal closure

To investigate the function of the *ALMT* gene family in stomata, we first compared the expression of each gene in *A. thaliana* guard cells and mesophyll. Among the 13 genes, *AtALMT12* was predominantly expressed in guard cells rather than mesophyll cells (**Fig. 1A**). This is similar to expression of two known guard cell channel genes, *SLAC1* and *KAT1*, and distinct from that of the gene for the mesophyll cell marker protein calmodulin-binding family protein (*CBP*). Interestingly, three transcripts (249, 335 and 412 bp) were detected by reverse transcription–PCR (RT–PCR) analysis using a pair of primers amplifying between exons 4 and 6 (**Fig. 2A** and **Supplementary Fig. S1**). Sequencing of these PCR products showed that they appeared to be splicing variants, produced by retaining intron 4, or both introns 4 and 5 (Reddy 2007). The predicted translation products give rise to truncated peptides [277 amino acids without exons 5 and 6, 324 amino acids without exon 6, compared with 560 amino acids for the complete open reading frame (ORF)] (**Supplementary Fig. S1B, C**).

To investigate expression further, we first used RT–PCR, which revealed a broad expression pattern throughout the plant (**Fig. 1B**). However, quantitative real-time RT–PCR showed that *AtALMT12* transcripts were 10-fold higher in shoots than in roots (**Fig. 1C**). Analysis of transgenic plants expressing the reporter gene, β-glucuronidase (GUS), under the

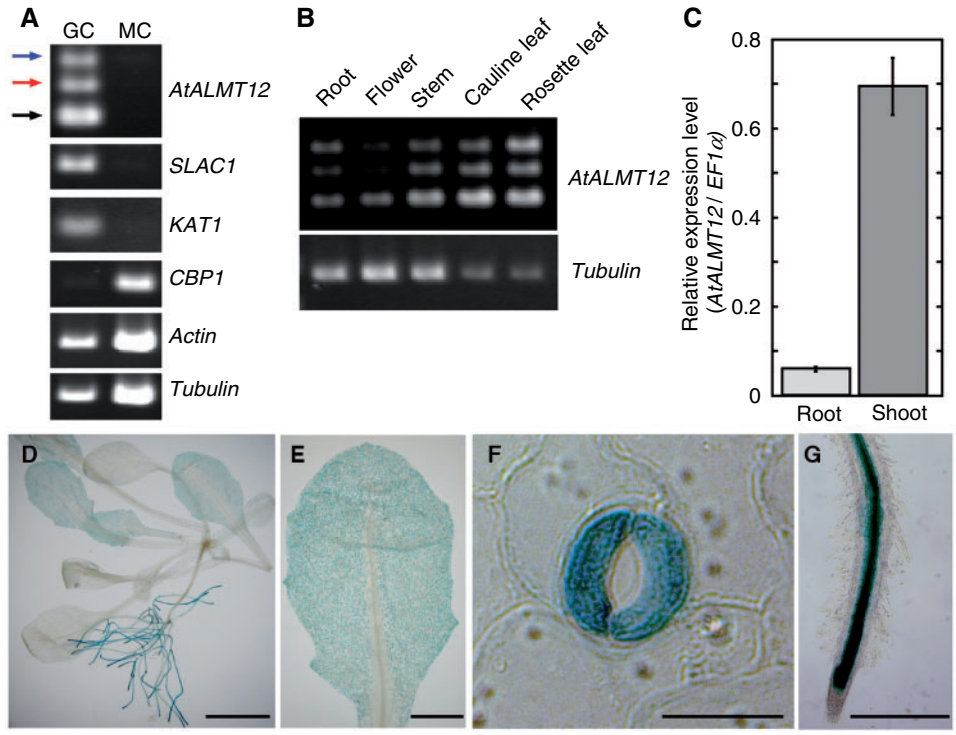

Fig. 1 AtALMT12 is expressed in guard cells. (A) The expression of *AtALMT12* (At4g17970), *SLAC1* (At1g12480), *KAT1* (At5g46240), *CBP* (At4g33050), *actin* (At5g09810) and β-*tubulin* genes (AT1g75780, AT5g62690, AT5g62700 and AT5g44340) in guard cells (GC) and mesophyll cells (MC) was detected by RT–PCR. Note that three amplification products are detected for *AtALMT12* (249 bp, black arrowhead; 335 bp, red arrowhead; 412 bp, blue arrowhead). (B) Comparison of the expression level of *AtALMT12* among plant organs. (C) Expression of *AtALMT12* determined by real-time PCR using primer set #2 (see **Fig. 2A**). Plants (Columbia) were grown in hydroponic medium and RNA was isolated from whole seedlings. Relative expression levels were normalized against the values of the *EF1α* transcript (At5g60390). Bars show the mean ± SEM ($n = 3$). (D–G) GUS reporter expression in seedling (D), leaf (E), guard cell (F) and root (G). GUS is driven by the region 3,157 bp upstream of the start codon. Bars = 5 mm (D), 1 mm (E), 20 μm (F) and 500 μm (G).

control of the putative *AtALMT12* promoter (3,157 bp upstream of the first ATG) showed that roots were stained largely in the vascular stele but that leaves were stained principally in guard cells (**Fig. 1D–G**).

To analyze the function of AtALMT12, we obtained two *AtALMT12* knock-down lines (*atalmt12-1*, WiscDsLox_329D04; and *atalmt12-2*, SALK_098126). In these lines, the T-DNA was inserted around 750 bp upstream from the start codon (**Fig. 2A**) and resulted in a significant reduction of transcript in leaves (**Fig. 2B**). As the phenotypes of the lines were indistinguishable (**Supplementary Fig. S2A**), we present data here for *atalmt12-1*.

Intact *atalmt12-1* plants had a wilty phenotype, consistent with impaired stomatal regulation (**Fig. 2C**). In this line, stomatal closure was suppressed in response to darkness, calcium and exogenous ABA (**Fig. 2D–F**). The F_1 progeny from a cross of the wild type and *atalmt12-1* had both wild-type morphology and sensitivity to ABA, indicating that the mutant is recessive (data not shown). Also implicating impaired stomatal closure, the average aperture in dark-adapted leaves was larger in

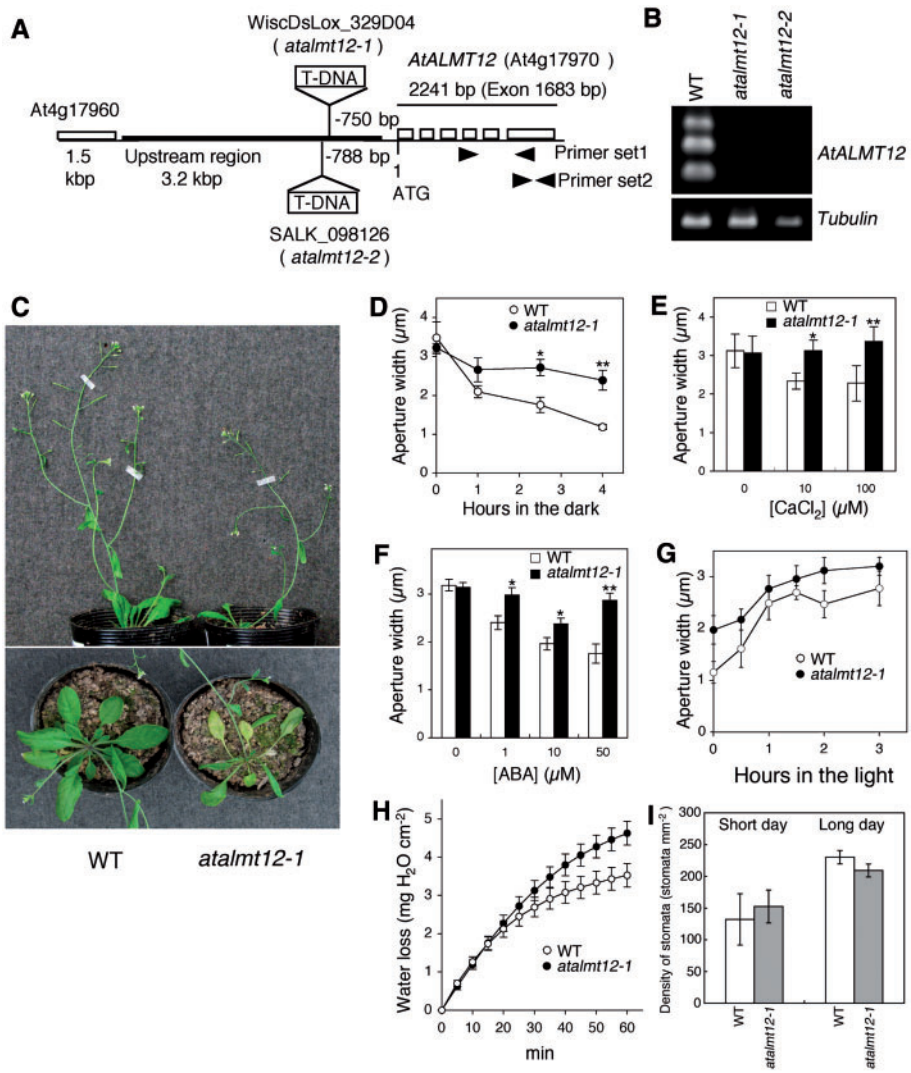

Fig. 2 Knockdown mutation of *AtALMT12* impairs stomatal responses and has a wilty phenotype. (A) Schematic of the *AtALMT12* locus (At4g17970) showing T-DNA insertion sites and primer locations (arrowheads) for RT–PCR analysis. (B) RT–PCR analysis using primer set #1 (or β-*tubulin* primers). (C) One-week-old wild-type (WT) and *atalmt12-1* plants were subjected to water withholding for a further 2 weeks. Photographs of representative plants from three independent replicates were taken from the side and top. (D) Dark-induced stomatal closure ($n = 4$ experiments). (E) Calcium-induced stomatal closure ($n = 4$ experiments). (F) ABA-induced stomatal closure ($n = 10$ experiments for 0, 1 and 10 μM ABA; $n = 4$ experiments for 50 μM ABA). For D–F, 20 stomata were measured for each genotype in each experiment, and symbols or bars plot the mean ± SEM. (G) Light-induced stomatal opening in the *atalmt12-1* mutant ($n = 5$ experiments). (H) Water loss of detached leaves ($n = 3$). Symbols plot the mean ± SEM. (I) Stomatal density. Plants were grown under short days (8L:16D) for 3 months or long days (16L:8D) for 3 weeks. Data are presented as the mean ± SD ($n = 5$ leaves). Differences from WT values were significant at $*P < 0.05$ and $**P < 0.01$, respectively.

atalmt12-1 than in the wild type (**Fig. 2G**, time zero). In contrast, stomata in *atalmt12-1* opened in response to light with similar kinetics to those of the wild type (**Fig. 2G**), suggesting that AtALMT12 is required for stomatal closure but not for opening.

From excised leaves, the rate of water loss over the first 20 min was indistinguishable between the genotypes (**Fig. 2H**). However, over longer times, as the leaves became dehydrated, the wild type lost water more slowly than did *atalmt12-1*; for example, between 40 to 60 min, the rates of water loss were 19.6±2.1 and 34.6±2.0 μg H_2O cm^{-2} min^{-1} for the wild type and *atalmt12-1*, respectively (with equivalence of these mean rates being rejected at $P < 0.01$). These results suggest that the stomata of *atalmt12-1* are defective in drought-induced closure, in agreement with their relatively low sensitivity to ABA. Taken together with the comparable density of stomata on the leaves of the two genotypes (**Fig. 2I**), our findings imply that AtALMT12 is involved in the control of stomatal closure under darkness and water-deficient conditions.

To determine whether the T-DNA insertion was responsible for the phenotypes, we stably transformed *atalmt12-1* with the wild-type gene, using either a 2,241 bp genomic sequence that spans the coding regions or the same sequence fused with green fluorescent protein (GFP) at the C-terminus, or the coding sequence fused to 3,157 bp of upstream sequence (**Fig. 2A** and **Supplementary Fig. S1**). Stomata in transformants with the genomic sequences with or without GFP, or with the coding sequence had a restored sensitivity to ABA (**Fig. 3** and **Supplementary Fig. S3**).

Because *atalmt12-1* plants were complemented by an *AtALMT12* genomic construct containing GFP (**Fig. 3**), we examined them to assess localization; however, GFP fluorescence was undetectable (data not shown). We also ran immunoblots to detect the protein, probing a crude microsomal fraction prepared from isolated guard cells with antisera against either GFP or an AtALMT12 peptide; again, AtALMT12 was undetectable, in both the wild type and the transgenics expressing *AtALMT12* from the native promoter. Therefore, to localize AtALMT12, the *AtALMT12* coding sequence was fused to GFP under the control of the cauliflower mosaic virus (CaMV) 35S promoter, and transiently expressed by particle bombardment in onion epidermal cells and in *Vicia faba* guard cells (**Fig. 4**). Fluorescence from the GFP fusion protein was observed on endomembranes, as seen by it surrounding the nucleus and co-localization with defined markers, and at the plasma membrane as judged by plasmolysis.

Electrophysiological analysis of AtALMT12

To determine the electrophysiological properties of AtALMT12, we used two-electrode voltage–clamp recording in a heterologous expression system (*Xenopus laevis* oocytes), where the AtALMT12 (coding sequence)::sGFP is predominantly localized to the plasma membrane (**Supplementary Fig. S4A**). *AtALMT12*-expressing oocytes showed large outward currents when sodium chloride was present in the bathing solution (**Fig. 5A**).

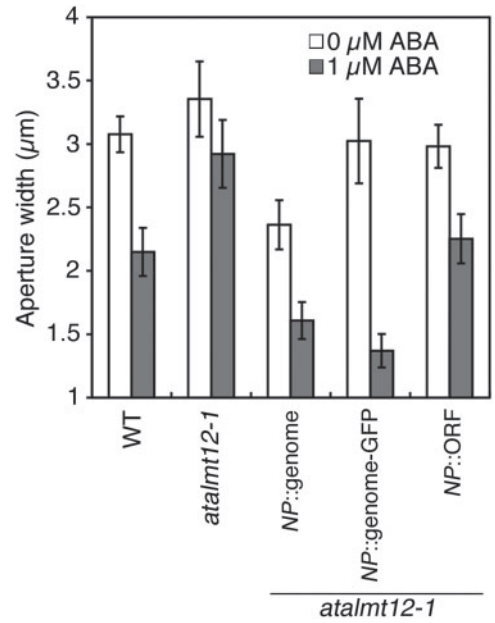

Fig. 3 Complementation of the ABA-insensitive phenotype of *atalmt12-1* with genomic *AtALMT12* sequences. Plants were treated with or without 1 μM ABA and stomatal closure was assayed. Complementation of *atalmt12-1* by the native promoter (NP)-driven genomic sequence of *AtALMT12* with or without GFP fusion (*NP*::genome, *NP*::genome–GFP; $n = 5–6$ independent experiments), and the NP-driven coding sequence (*NP*::ORF, $n = 8$ independent experiments).

Decreasing the extracellular concentration reduced the outward current, but replacing sodium chloride by other chloride salts did not affect the outward current (**Fig. 5B** and **Supplementary Fig. S4B**), demonstrating that AtALMT12 is an anion channel permeable to chloride. Although the related transporters, TaALMT1 and ZmALMT1, carry both inward and outward currents (Piñeros et al. 2008a, Piñeros et al. 2008b), AtALMT12 gave rise to little if any inward current as extracellular chloride concentrations were changed (**Fig. 5A, B**), implying that AtALMT12 is an outward rectifier, at least when expressed in oocytes.

Furthermore, TaALMT1 is permeable to several ions, including the eponymous malate, as well as chloride, nitrate and sulfate (Piñeros et al. 2008a, Zhang et al. 2008), whereas AtALMT12 was more permeable to nitrate than chloride but scarcely permeable to malate or sulfate (**Fig. 5C**). In addition, when cultured tobacco cells were transformed with the *AtALMT12* coding sequence under the control of the 35S promoter, no malate exclusion was detected (data not shown), in contrast to TaALMT1 (Sasaki et al. 2004). These results confirm that the ion selectivity of AtALMT12 is distinct from that of TaALMT1.

We also examined the effect of aluminum on AtALMT12, since aluminum-dependent activation is a specific feature of both TaALMT1 and AtALMT1 (Sasaki et al. 2004, Hoekenga et al. 2006). Extracellular aluminum (100 μM $AlCl_3$) slightly enhanced outward currents at +80 mV (8.6±5.2%, $n = 12$), but

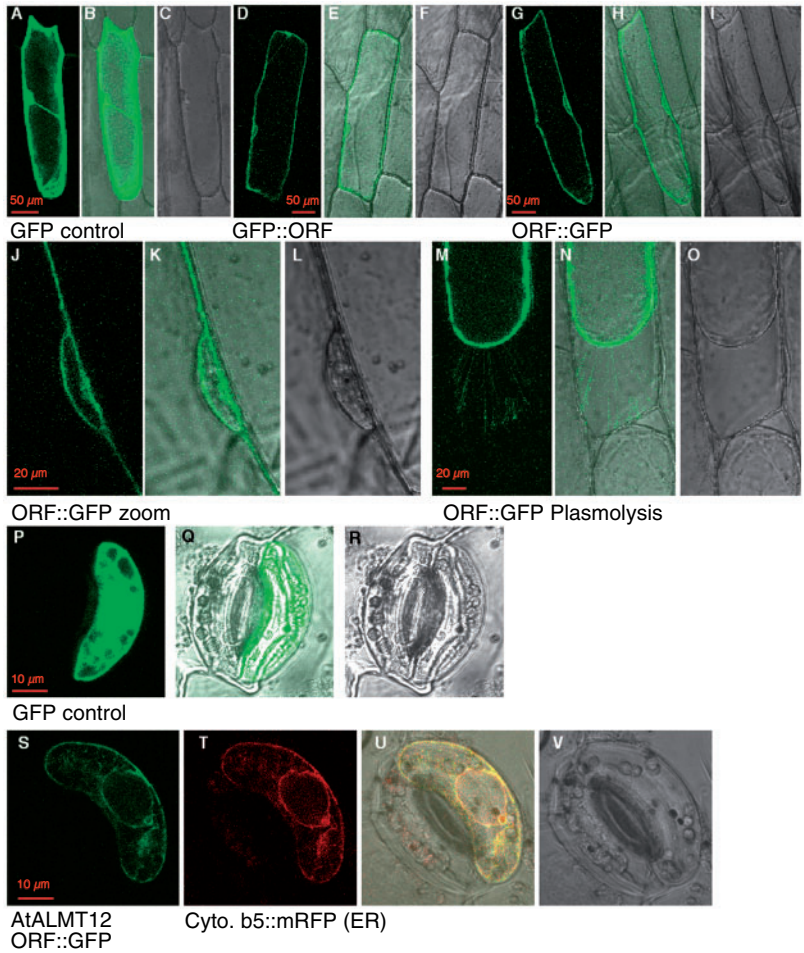

Fig. 4 Localization of AtALMT12. The *AtALMT12* coding sequence–*GFP* (ORF::GFP) construct under the control of the 35S promoter was transiently expressed in onion epidermal cells (A–O) and *V. faba* guard cells (P–V). As control, GFP alone was expressed in onion cells (A–C) or *V. faba* cells (P–R). Expression of GFP::AtALMT12 (N-terminal fusion, D–F) or AtALMT12::GFP (C-terminal fusion, G–I) shows similar localizations in onion cells. GFP fluorescence surrounds the nucleus, suggesting that AtALMT12 localized to both endomembranes and plasma membrane (J–L). Plasmolysis of AtALMT12::GFP-expressing cells with 1 M mannitol shows that the Hechtian strands attaching the plasma membrane to the cell wall are labeled, confirming that the protein is localized on the plasma membrane. Co-expression of AtALMT12::GFP with Cyt b5::mRFP as an ER marker (S–V). Fluorescence from AtALMT12::GFP co-localized with Cyt b5::mRFP suggests that AtALMT12 is targeted to the ER. Photographs show GFP fluorescence images (A, D, G, J, M, P, S), mRFP images (T), transmitted light images (C, I, L, O, R, V) and merged images (B, E, H, K, N, Q, U).

this effect is far smaller than for TaALMT1 ($139.3 \pm 68.2\%$, $n = 9$), indicating that AtALMT12 possesses a negligible response to aluminum.

To examine whether the splice variants also encode active anion channels, we expressed them in *Xenopus* oocytes. Neither variant gave rise to currents distinguishable from water-injected control (**Fig. 5D**), despite their being detected at the oocyte crude membrane in immunoblots (**Supplementary Fig. S4C**). These results suggest that the splice variants are not functional as anion transporters.

Plasma membrane anion channels play essential roles in stomatal movement (Ward et al. 2009). For example, the *slac1* mutation disrupts both calcium- and ABA-dependent S-type anion currents and stomatal responses, but alters currents from neither R-type anion channels nor calcium-permeable channels (Vahisalu et al. 2008). The fact that stomatal closure was impaired in *atalmt12-1* led us to measure both R- and S-type anion currents in guard cells by the whole-cell patch–clamp technique (Mori et al. 2006, Munemasa et al. 2007). Elevated extracellular calcium (40 mM) or ABA (10 or 50 μM) activated S-type anion currents in *atalmt12-1* guard cell protoplasts, to a similar extent as in the wild type (**Fig. 6A–E**). As a control, calcium activation of an S-type anion current was assayed in *cpk6-1* and was absent, as reported previously (Mori et al. 2006). Similarly, significant differences in R-type anion currents between the wild type and *atalmt12-1* were absent (**Fig. 6F, G**). These results imply that *AtALMT12* encodes neither R-type nor S-type anion channels.

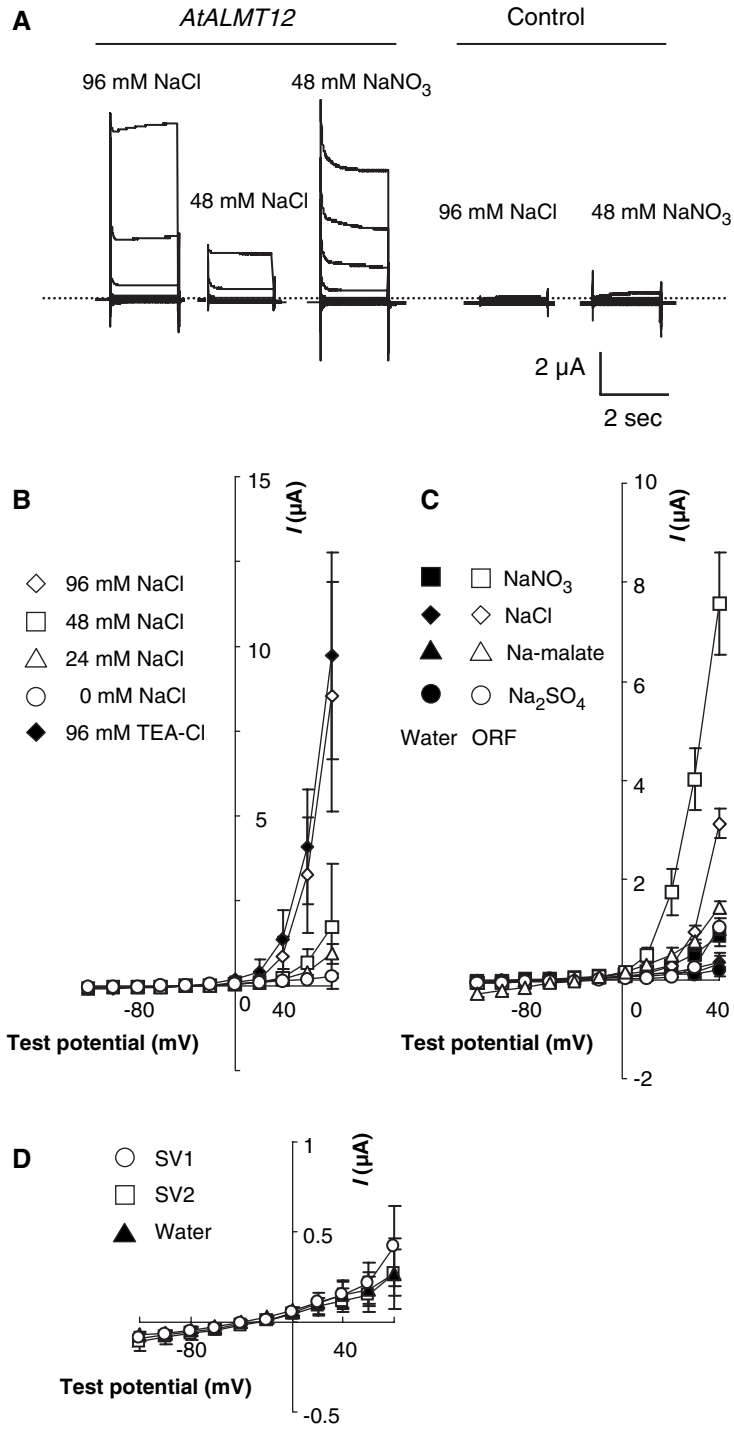

Fig. 5 Electrophysiological properties of *AtALMT12* expressed in *Xenopus* oocyte plasma membranes. (A) Typical traces of anion currents across the plasma membrane in oocytes expressing *AtALMT12* (ORF) (left) and water-injected controls (right). The dotted line indicates zero current level (±0 nA). (B) Mean current–voltage relationships in *AtALMT12* (ORF)-expressing oocytes recorded with a range of extracelluar NaCl concentrations [96 mM ($n = 23$), 48 mM ($n = 12$), 24 mM ($n = 11$), 0 mM ($n = 11$) and 96 mM TEA-Cl ($n = 11$)]. (C) Current–voltage relationships for *AtALMT12*-expressing (ORF: open symbols) and water-injected control (water: filled symbols) oocytes recorded with various anions ($n = 4$ for each solution). (D) Current–voltage relationships for oocytes expressing the splicing variant SV1 ($n = 10$) and SV2 ($n = 12$) and water-injected controls ($n = 10$). All symbols plot the mean ± SEM.

Discussion

The ALMT family was originally identified in wheat, with the characterization of TaALMT1 in conferring aluminum resistance (Sasaki et al. 2004). Subsequent reports demonstrated that TaALMT1 transported malate, chloride, nitrate and sulfate (Pineros et al. 2008a, Zhang et al. 2008). While the maize homolog, ZmALMT1, is permeable to the inorganic anions rather than malate, it is neither activated by aluminum nor related to aluminum resistance (Pineros et al. 2008b). In *A. thaliana*, AtALMT1 has been characterized as an aluminum-activated malate transporter and involved in aluminum resistance (Hoeckenga et al. 2006, Kobayashi et al. 2007), although it is still unknown whether it transports inorganic anions. Another family member in *A. thaliana*, AtALMT9, is a malate transporter localized on vacuolar membrane and involved in

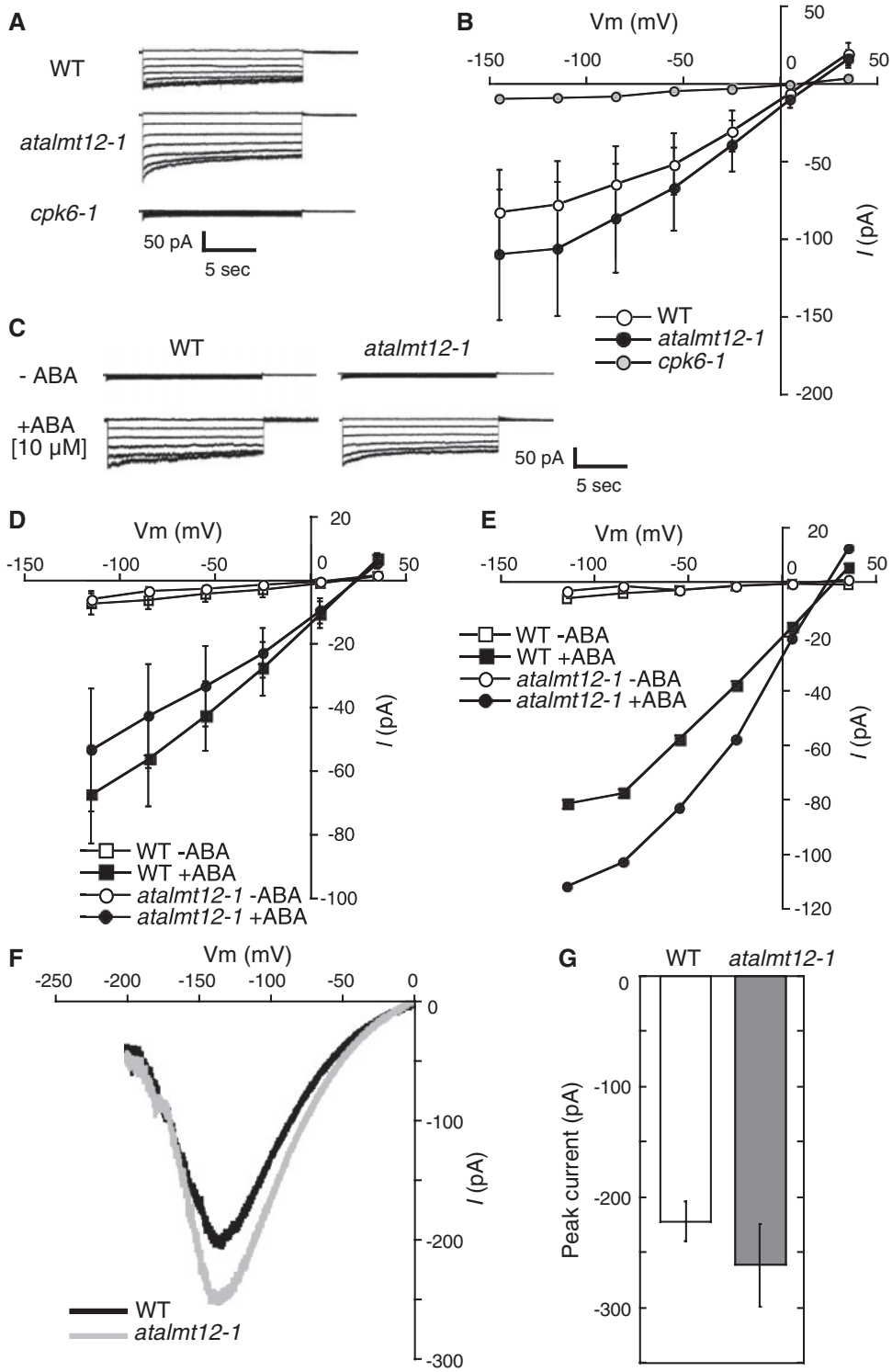

Fig. 6 S-type and R-type anion currents in *A. thaliana* guard cell protoplasts. (A, B) Whole-cell S-type anion currents in response to a high extracellular calcium concentration (40 mM $CaCl_2$ in the bath solution). (A) Representative traces of calcium-activated S-type anion currents. (B) Current–voltage relationships of the wild type ($n = 6$), *atalmt12-1* ($n = 6$) and *cpk6-1* ($n = 3$). (C–E) Whole-cell S-type anion currents with 10 μM (C, D) or 50 μM (E) ABA in the bath solution. (C) Representative traces of S-type anion currents. (D) Current–voltage relationships of the wild type ($n = 5$) and *atalmt12-1* ($n = 7$). (E) Current–voltage relationship of the wild type and *atalmt12-1* ($n = 2$). (F) Representative traces of R-type anion currents in the wild-type and *atalmt12-1*. (G) Average peak R-type anion channel current in the wild type ($n = 4$) and *atalmt12-1* ($n = 3$). All data are the mean ± SEM. Significant differences (Student's *t*-test) were not observed between the wild type and *atalmt12-1* in both the S-type anion current (E; $P = 0.587$ at −115 mV) and the R-type anion current (F; $P = 0.348$ at negative peak values).

cytosolic malate homeostasis (Kovermann et al. 2007). These findings suggest that the ALMT proteins comprise a diverse family of anion channels and transporters, possessing multiple functions.

Our results add stomatal aperture control to the list of functions handled by aluminum-activated malate transporter family members. AtALMT12 functions in mediating stomatal closure rather than in conferring aluminum resistance. The loss-of-function mutant has a wilty phenotype and closes its stomata sluggishly in response to dehydration, calcium or ABA.

An ambiguity involving AtALMT12 function concerns its subcellular localization. We failed to detect the protein when driven by the native promoter in a homologous system, implying that its endogenous expression level is low. However, when driven by the 35S promoter in transient, heterologous systems, AtALMT12 was observed at both the plasma membrane and endomembranes. It is difficult to evaluate the significance of these observations for the function of AtALMT12 because the localization of transporters is often surprisingly dynamic, reflecting an important level of regulation. For example, in *A. thaliana* guard cells, KAT1, an inward-rectifying potassium channel, is triggered by ABA to relocate from the plasma membrane to endosomes, thereby quickly decreasing the capacity for potassium flux (Sutter et al. 2007). As another example, also from *A. thaliana*, trafficking of a boron transporter, BOR1, from the plasma membrane to endosomes is regulated by boron availability, presumably to preserve optimal boron status (Takano et al. 2005). Until AtALMT12 can be detected when expressed at endogenous levels, the role of subcellular localization changes for the regulation of its function must be conjectural.

When stomata close, turgor pressure decreases and this is accompanied by a major efflux of solutes (Ward et al. 2009). Here, AtALMT12 in the oocyte expression system catalyzed outward-rectifying currents, which reflects an influx of anions across the plasma membrane of the oocyte (**Fig. 5A–C**), a direction opposite to what is expected for stomatal closure. One of the possible explanations could be that the AtALMT12 transporter releases anions into the cytosol from the endoplasmic reticulum (ER) or vacuole by the outward-rectifying currents. It might be helping to provoke the massive solute efflux via the anion channels on the plasma membrane needed for stomatal closure. Another explanation is that the direction of current flow through AtALMT12 located on the plasma membrane is regulated by a protein factor missing from oocytes. Consistent with this idea, the SLAC1-mediated S-type anion channel activity is up-regulated by phosphorylation with the open stomata 1 (OST1) protein kinase and down-regulated by dephosphorylation with group A-type 2C protein phosphatases (Geiger et al. 2009, Lee et al. 2009). In *Xenopus* oocytes, co-expression of SLAC1 and OST1 correlates with the ability of chloride and nitrate to efflux across the plasma membrane. Whether these pathways also regulate AtALMT12 function, especially for inward-rectifying currents, remains to be determined.

It has been suggested that at least one signaling pathway, in addition to the one mediated by S-type anion channels such as SLAC1, is involved in ABA-induced stomatal closure (Pandey et al. 2007). We hypothesize that the target of this pathway is AtALMT12, which possesses a high capacity for the transport of nitrate and chloride and substantially abrogates stomatal aperture response when knocked-down. Further study of AtALMT12 together with SLAC1, AtABCB14 and AtNRT1.1/CHL1 will enhance our understanding of the molecular mechanisms for stomatal movements (Guo et al. 2003, Lee et al. 2008, Negi et al. 2008, Saji et al. 2008, Vahisalu et al. 2008), and the study of the ALMT transporter family might reveal how transporters evolve new functions.

Materials and Methods

Plant materials and growth conditions

Arabidopsis thaliana L. Heynh was used for experiments, and all lines are in the Columbia background. Knockdown mutant lines *atalmt12-1* (WiscDsLox_329D04) and *atalmt12-2* (SALK_098126) were obtained from the Arabidopsis Biological Resource Center (Ohio University). T-DNA insertion and homozygous lines were selected by PCR using the T-DNA left border-specific primers, p745: 5′-AACGTCCGCAATGTGTTA TTAAGTTGTC-3′ for the WiscDsLox line or LBa1: 5′-TGGTT CACGTAGTGGGCCATCG-3′ for the SALK line, and the gene-specific primers, forward primer: 5′-CTCAGTTCTCGATGTACC TAC-3′ and reverse primer: 5′-GAATCTCTTGTAGGTTCGA GT-3′. Plants were grown on soil or hydroponic culture medium [one-sixth Murashige and Skoog (MS) medium supplemented with 1% sucrose] under 16 or 8 h light conditions (40–100 μmol m^{-2} s^{-1}) at 20–22°C. For hydroponics, seeds were surface-sterilized in 70% ethanol followed by 0.25% sodium hypochlorite containing 0.05% Tween-20.

RT–PCR

Total RNA was extracted from plant materials using RNeasy Plant Mini kits (Qiagen K.K., Tokyo, Japan) or TRIzol reagent (Invitrogen, Carlsbad, CA, USA). Guard and mesophyll cell protoplasts were isolated enzymatically from leaves using a method described previously (Kwak et al. 2003). Total RNA from leaves, stems and flowers was prepared from plants grown on soil; the RNA from roots was prepared from seedlings grown on mesh in hydroponics. Prior to RT–PCR, RNA samples were treated with DNase (RQ1 RNase-Free DNase, Promega, Madison, WI, USA) to remove contaminating genomic DNA. First-strand cDNA synthesis was performed in a 20 μl reaction mixture containing 1 μg of total RNA and oligo(dT) primers using the SuperScript First-Strand Synthesis system for RT–PCR (Invitrogen). RT–PCR was performed using ExTaq polymerase (TAKARA BIO INC., Ohtsu, Japan). The primers for semi-quantitative amplification of *AtALMT12* (249, 335 and 412 bp) are 5′-CAGATTCAAAAGACAGAATCTACG-3′ and 5′-GATC TTTAAAAAGCGCGCGAACGGAT-3′, which are designed for

exon 4 and 6 (primer set #1 in **Fig. 2A**). The primers used as the guard cell-specific genes are: 5′-TGCTCGGATCAATTTCTTCA-3′, 5′-GATGCGACTCTTCCTCTGCT-3′ for *SLAC1* (At1g12480, 377 bp) (Saji et al. 2008); 5′-AAGCATGGGATGGGAAGAG TGG-3′, 5′-CCATTAGAGCAGTGTCGGAAGT-3′ for *KAT1* (At5g46240, 89 bp) (Mori et al. 2006); and 5′-GTTATATTAGT GGTCATGGGTCTTG-3′, 5′-CCTGTAACTCTTGTACACCTTTT GT-3′ for the mesophyll-specific gene, *CBP* (At4g33050, 378 bp) (Mori et al. 2006). The primers used for internal control genes are: 5′-CCTGATAACTTCGTCTTTGG-3′, 5′-GTGAACT CCATCTCGTCCAT-3′ for β-tubulins (968 bp, AT1G75780, AT5G62690, AT5G62700 and AT5G44340) (Knight et al. 1999); and 5′-GGCCGATGGTGAGGATATTCAGCCACTTG-3′, 5′-TCGATGGACCTGACTCATCGTACTCACTC-3′ for actin (At5g09810, 1,109 bp) (Mori et al. 2006). The amplified PCR products were resolved by agarose gel electrophoresis, and then imaged by ethidium bromide staining.

For quantitative real-time RT–PCR, levels of *AtALMT12* and *EF1α* transcripts were determined on the LightCycler instrument (Roche Diagnostics, Mannheim, Germany) with the THUNDERBIRD SYBR qPCR Mix (TOYOBO, Osaka, Japan). The primers 5′-CATCTCCACGTGGCACTTCAAGAT-3′ and 5′- CAGTCCTAAAGCTTGAAAGTGAAAC-3′ amplified a 271 bp fragment of the *AtALMT12* gene (primer set #2 in **Fig. 2A**). To amplify the *EF1α* (At5g60390) transcript (103 bp), primers 5′-CCTTGGTGTCAAGCAGATGA-3′ and 5′-TGAAGACACCTCC TTGATGATTT-3′ were designed as described previously (Takano et al. 2006). Reaction conditions for thermal cycling were: 95°C for 30 s, 40 cycles of 95°C for 5 s, and 60°C for 30 s. For each gene, a standard curve was prepared using a serial dilution of the reverse-transcribed cDNA sample. Taking into account the differences in total RNA present in each sample, the amount of *AtALMT12* transcript was normalized to the amount of *EF1α* transcript detected in the same sample.

Construction of binary plasmids and transformation of plants

For construction of plasmids, PCR was performed using the high fidelity enzyme Prime STAR HS or GXL DNA polymerases (TAKARA BIO INC.). To amplify the 3,157 bp genomic sequence upstream of *AtALMT12*, the primers were used as follows. Forward primer: 5′-aaccaattcagtcgacGCAGTCTTGCAGACAT ATTAGCGAG-3′ and reverse primers: 5′-aagctgggtctagatatctct agaTTTGAGGGAGAGAAATTGGTACTCTC-3′ or 5′-aagctgggt ctagatatccctaggTTTGAGGGAGAGAAATTGGTACTCTC-3′. These primers are designed for In-Fusion cloning and include restriction endonuclease site sequences (underlined). The fragments were cloned into the pENTR 3C entry plasmid (Invitrogen) using the In-Fision 2.0 Dry-Down PCR cloning kit (Clontech–TAKARA BIO INC.). The construction of the *AtALMT12* promoter::GUS reporter gene was performed using the pGWB3 plasmid (Nakagawa et al. 2007) via the Gateway Cloning system (Invitorgen). The *AtALMT12* genomic fragment of 2,241 bp and the 1,684 bp ORF (coding sequence) were amplified using primers 5′-GCgtcgactctagaATGTCCAATAAGGTTCACGTAGG GAGC-3′ and 5′-CCgagctcTCATTCCGCGGCACCGACACTG ATCGT-3′ (for the stop codon), and 5′-CGccatggACCCTCCG CCACCTTCCGCGGCACCGACACTGATCGT-3′ (for fusion of C-terminal GFP), which include restriction sites (underlined). Binary plasmids of the *AtALMT12* promoter fused to the coding sequence, genomic sequence or genomic sequence::GFP were modified from the *AtALMT12* promoter::GUS reporter gene plasmid using pGWB3 by replacing the GUS gene with the *AtALMT12* fragments. The binary plasmids under the control of the CaMV 35S promoter were constructed using pIG121-Hm (Ohta et al. 1990). For transient expression of AtALMT12::GFP or GFP::AtALMT12 constructs under the control of the CaMV 35S promoter, the plasmids pTH2 (Chiu et al. 1996) or pGWB2 (Nakagawa et al. 2007) were used, with modification.

The binary plasmids were introduced into *Agrobacterium tumefaciens* strain EHA101 (Hood et al. 1986). Transformations were performed as described previously (Clough and Bent 1998). Transgenic plants (T_1) were selected on Murashige–Skoog (MS) medium containing 20 μg ml^{-1} kanamycin and 100 μg ml^{-1} carbenicillin, and then grown in soil. The self-pollinated progeny (T_2) were selected by kanamycin resistance and analyzed for expression of *ALMT1* and measurement of stomatal apertures. Transformation of tobacco cells was carried out as described previously with minor modifications (An 1985, Sasaki et al. 2004).

The AtALMT12::GFP fusion under the CaMV 35S promoter was transiently transformed into onion epidermal cells and *V. faba* guard cells by particle bombardment (PDS-1000, Bio-Rad Laboratories, Hercules, CA, USA). For co-localization analysis in *V. faba* cells, the construct of the Cyt b5::monomeric red fluorescent protein (mRFP) was used as an ER marker (Toyooka et al. 2006). Fluorescence was observed on a Zeiss confocal microscope (LSM510 Carl Zeiss, Oberkochen, Germany), with 488 nm excitation from an argon laser and a 505–530 nm bandpass filter for GFP, and 543 nm excitation from an He–Ne laser and a 560–615 nm bandpass filter for mRFP.

GUS staining

A stable transgenic plant expressing *GUS* under the *AtALMT12* native promoter control was used for GUS staining by a method described previously (Weigel and Glazebrook 2002).

Stomatal aperture measurements

The width of stomatal apertures was measured as described previously (Mori et al. 2006). Excised rosette leaves from 4- to 5-week-old plants were floated on opening buffer (5 mM KCl, 50 μM $CaCl_2$ and 10 mM MES-Tris, pH 5.7) for 2 h at 22°C under illumination from a fluorescent lamp at a photon flux of 100 μmol m^{-2} s^{-1}, to open stomata. Leaves were floated for another 2 h after addition of ABA to the opening buffer. For measuring calcium-induced stomatal closure, $CaCl_2$ was omitted from the opening buffer. For dark-induced stomatal closure, the Petri dish containing leaves was wrapped with aluminum foil at 2 h, then further incubated for the indicated periods.

Electrophysiology using *X. laevis* oocytes

For expression in oocytes, cRNAs were prepared using a MEGA script kit with cap analog (Ambion, Austin, TX, USA) from linearized (*Bam*HI-digested) pXBG-AtALMT12 plasmid DNA, which also contained the coding region of a *Xenopus* β-globin gene (Preston et al. 1992). Female *X. laevis* were purchased from Hamamatsu Seibutsu Kyozai Co. (Hamamatsu, Japan). Stage V–VI defolliculated oocytes were isolated and used for experiments. Oocytes were injected with 50 nl of water containing 40 ng of cRNA (or 50 nl of water for controls) using a microinjection system (NANOJECT II, Drummond Scientific Co., Broomall, PA, USA). The oocytes were stored at 18°C in modified Barth's solution [88 mM NaCl, 1 mM KCl, 2.4 mM $NaHCO_3$, 0.33 mM $Ca(NO_3)_2$, 0.41 mM $CaCl_2$, 0.82 mM $MgSO_4$, 20 mM HEPES-Tris (pH 7.5), 50 μg ml^{-1} gentamycin] before and after microinjection. Recordings were obtained 2 d after microinjection with MEZ-7200 and CEZ-1200 amplifiers equipped with the SET-1201 step pulse generator (Nihon Kohden, Tokyo, Japan) to measure net currents across the oocyte membrane at different membrane voltages. The recording electrodes were filled with 3 M KCl. The basic bath solution contained 96 mM NaCl, 1 mM KCl, 1.8 mM $CaCl_2$, 0.1 mM $LaCl_3$ and 5 mM HEPES-NaOH (pH 7.5). The extracellular chloride concentration was adjusted by decreasing the NaCl, and the osmolarities of each test solution were adjusted to 210 mOsm kg^{-1} (equivalent to that of Barth's solution) with sorbitol. Currents were measured in response to voltage pulses from −120 to +80 mV in 20 mV increments, stepped from a holding potential of −60 mV with each 3 s interval. Current–voltage curves were constructed from the steady-state currents.

Patch–clamp experiments

For whole-cell patch–clamp recordings of S-type and R-type anion currents, *A. thaliana* guard cell protoplasts were prepared from rosette leaves of 4- to 6-week-old plants by an enzymatic method, as previously described (Pei et al. 1997). Whole-cell currents were recorded as previously described (Munemasa et al. 2007). For S-type anion current measurements, the patch–clamp solutions contained 150 mM CsCl, 2 mM $MgCl_2$, 6.7 mM EGTA, 5.58 mM $CaCl_2$ (free Ca^{2+} concentration: 2 μM), 5 mM ATP and 10 mM HEPES-Tris (pH 7.1) in the pipet and 30 mM CsCl, 2 mM $MgCl_2$, 1 mM $CaCl_2$ and 10 mM MES-Tris (pH 5.6) in the bath (Pei et al. 1997). The concentration of free calcium was calculated using the 'CALCIUM' program (Foehr et al. 1993). To measure R-type anion channel currents, the pipet solution contained 75 mM K_2SO_4, 2 mM $MgCl_2$, 5 mM EGTA, 2.5 mM $CaCl_2$ and 10 mM HEPES-Tris (pH 7.1). The bath solution contained 50 mM $CaCl_2$, 2 mM $MgCl_2$ and 10 mM MES-Tris (pH 5.6) (Mori et al. 2006). Osmolality was adjusted to 500 mmol kg^{-1} (pipet solutions) and 485 mmol kg^{-1} (bath solutions) with sorbitol. In S-type anion channel recording, membrane voltage was clamped from +35 to −145 mV (for calcium-activated currents) or to −115 mV (for ABA-activated currents) with 30 mV decrements. The holding potential was +30 mV. For R-type anion channel recording, the voltage was ramped from the holding potential of 0 mV to −200 mV with a ramp speed of −20 mV s^{-1}.

Immunoblot analysis

Crude microsomal membrane fractions of guard cells and oocytes were prepared as described previously (Sasaki et al. 2004, Yamaguchi et al. 2005, Ledc-Nadeau et al. 2007). The proteins were separated by SDS–PAGE and electroblotted onto a polyvinylidene difluoride filter. The filter was incubated with the anti-AtALMT12 antiserum raised against the synthetic polypeptide (C-EKTDSKDRIYEGYQA) or an anti-GFP antibody (TOYOBO). The antibody-bound antigen was detected using a protocol described previously (Sasaki et al. 2004, Yamaguchi et al. 2005).

Supplementary data

Supplementary data are available at PCP online.

Funding

This work was supported by the Ministry of Education, Culture, Sports, Science and Technology of Japan [Grant-in-Aid for Scientific Research (No. 17078007 to T.S., No. 17078006 to Y.M., Nos. 17380049, 18208008215800078 to Y.Y.)]; the Nissan Science Foundation [to I.C.M.]; Ohara Foundation for Agricultural Science.

Acknowledgments

We are grateful to the following for providing plasmids: T. Nakagawa (pGWB2, pGWB3), Y. Niwa (pTH2 plasmids), H. Sano and K. Nakamura (pIG121-Hm plasmid and *Agrobacterium* EHA101). We also thank M. Ariyoshi, Y. Tsuchiya, E. Himi and M. Fujii for experimental assistance, and T.I. Baskin for critical reading of the manuscript.

References

An, G. (1985) High efficiency transformation of cultured tobacco cells. *Plant Physiol.* 79: 568–570.

Chiu, W.-I., Niwa, Y., Zeng, W., Hirano, T., Kobayashi, H. and Sheen, J. (1996) Engineered GFP as a vital reporter in plants. *Curr. Biol.* 6: 325–330.

Clough, S.J. and Bent, A.F. (1998) Floral dip: a simplified method for *Agrobacterium*-mediated transformation of *Arabidopsis thaliana*. *Plant J.* 16: 735–745.

Delhaize, E., Gruber, B.D. and Ryan, P.R. (2007) The roles of organic anion permeases in aluminium resistance and mineral nutrition. *FEBS Lett.* 581: 2255–2262.

Foehr, K.J., Worchol, W. and Gratzel, M. (1993) Calculation and control of free divalent cations in solutions used for membrane fusion studies. *Methods Enzymol.* 221: 149–157.

Geiger, D., Scherzer, S., Mumm, P., Stange, A., Marten, I., Bauer, H., et al. (2009) Activity of guard cell anion channel SLAC1 is controlled by

drought-stress signaling kinase–phosphatase pair. *Proc. Natl Acad. Sci. USA* 106: 21425–21430.

Guo, F.-Q., Young, J. and Crawford, N.M. (2003) The nitrate tansporter AtNRT1.1 (CHL1) functions in stomatal opening and contributes to drought susceptibility in Arabidopsis. *Plant Cell* 15: 107–117.

Hedrich, R., Busch, H. and Raschke, K. (1990) Ca^{2+} and nucleotide dependent regulation of voltage dependent anion channels in the plasma membrane of guard cells. *EMBO J.* 9: 3889–3892.

Hoekenga, O.A., Maron, L.G., Piñeros, M.A., Cançado, G.M.A., Shaff, J., Kobayashi, Y., et al. (2006) *AtALMT1*, which encodes a malate transporter, is identified as one of several genes critical for aluminum tolerance in *Arabidopsis*. *Proc. Natl Acad Sci USA* 103: 9738–9743.

Hood, E.E., Helmer, G.L., Fraley, R.T. and Chilton, M.-D. (1986) The hypervirulence of *Agrobacterium tumefaciens* A281 is encoded in a region of pTiBo542 outside of T-DNA. *J. Bacteriol.* 168: 1291–1301.

Hosy, E, Vavasseur, A., Mouline, K., Dreyer, I., Gaymard F., Porée, F., et al. (2003) The *Arabidopsis* outward K^+ channel GORK is involved in regulation of stomatal movements and plants transpiration. *Proc. Natl Acad. Sci. USA* 100: 5549–5554.

Knight, H., Veale, E.L., Warren, G.J. and Knight, M.R. (1999) The *sfr6* mutation in Arabidopsis suppresses low-temperature induction of genes dependent on the CRT/DRE sequence motif. *Plant Cell* 11: 875–886.

Kobayashi, Y., Hoekenga, O.A., Itoh, H., Nakashima, M., Saito, S., Shaff, J.E., et al. (2007) Characterization of *AtALMT1* expression in aluminum-induced malate release and its role for rhizotoxic stress tolerance in Arabidopsis. *Plant Physiol.* 145: 843–852.

Kochian, L.V., Hoekenga, O.A. and Piñeros, M.A. (2004) How do crop plants tolerate acid soils? Mechanisms of aluminum tolerance and phosphorous efficiency. *Annu. Rev. Plant Biol.* 55: 459–493.

Kovermann, P., Meyer, S., Hörtensteiner, S., Picco, C., Scholz-Starke, J., Ravera, S., et al. (2007) The Arabidopsis vacuolar malate channel is a member of the ALMT family. *Plant J.* 52: 1169–1180.

Kwak, J.M., Mori, I.C., Pei, Z.-M., Leonhardt, N., Torres, M.A., Dangl, J.L., et al. (2003) NADPH oxidase *AtrbohD* and *AtrbohF* genes function in ROS-dependent ABA signaling in *Arabidopsis*. *EMBO J.* 22: 2623–2633.

Ledc-Nadeau, A., Lahjouji, K., Bissonnette, P., Lapoinate, J.-Y. and Bichet, D.G. (2007) Elaboration of a novel technique for purification of plasma membrane from *Xenopus laevis* oocytes. *Amer. J. Physiol. Cell Physiol.* 292: C1132–C1136.

Lee, M., Choi, Y., Burla, B., Kim, Y.-Y., Jeon, B., Maeshima, M., et al. (2008) The ABC transporter AtABCB14 is a malate importer and modulates stomatal response to CO_2. *Nature Cell Biol.* 10: 1217–1223.

Lee, S.C., Lan, W., Buchanan, B.B. and Luan, S. (2009) A protein kinase–phosphatase pair interacts with an ion channel to regulate ABA signaling in plant guard cells. *Proc. Natl Acad. Sci. USA* 106: 21419–21424.

Ma, J.F., Ryan, P.R. and Delhaize, E. (2001) Aluminium tolerance in plants and the complexing role of organic acids. *Trends Plant Sci.* 6: 273–278.

Mori, I.C., Murata, Y., Yang, Y., Munemasa, S. Wang, Y.-F., Andreoli, S., et al. (2006) CDPKs CPK6 and CPK3 function in ABA regulation of guard cell S-type anion- and Ca^{2+}-permeable channels and stomatal closure. *PLoS Biol.* 4: e327.

Munemasa, S., Oda, K., Watanabe-Sugimoto, M., Nakamura, Y., Shimoishi, Y. and Murata, Y. (2007) The coronatine-insensitive 1 mutation reveals the hormonal signaling interaction between abscisic acid and methyl jasmonate in Arabidopsis guard cells. Specific impairment of ion channel activation and second messenger production. *Plant Physiol.* 143: 1398–1407.

Nakagawa, T., Kurose, T., Hino, T., Tanaka, K., Kawamukai, M., Niwa, Y., et al. (2007) Development of series of gateway binary vectors, pGWBs, for realizing efficient construction of fusion genes for plant transformation. *J. Biosci. Bioeng.* 104: 34–41.

Negi, J., Matsuda, O., Nagasawa, T., Oba, Y., Takahashi, H., Kawai-Yamada, M., et al. (2008) CO_2 regulator SLAC1 and its homologues are essential for anion homeostasis in plant cells. *Nature* 452: 487–491.

Ohta, S., Mita, S., Hattori, T. and Nakamura, K. (1990) Construction and expression in tobacco of a β-glucuronidase (GUS) reporter gene containing an intron within the coding sequence. *Plant Cell Physiol.* 31: 805–813.

Pandey, S., Zhang, W. and Assmann, S.M. (2007) Roles of ion channels and transporters in guard cell signal transduction. *FEBS Lett.* 581: 2325–2336.

Pei, Z.M., Kuchitsu, K., Ward, J.M., Schwarz, M. and Schroeder, J.I. (1997) Differential abscisic acid regulation of guard cell slow anion channels in Arabidopsis wild-type and abi1 and abi2 mutants. *Plant Cell* 9: 409–423.

Pilot, G., Lacombe, B., Gaymard, F., Chérel, I., Boucherez, J., Thibaud, J.-B., et al. (2001) Guard cell inward K^+ channel activity in *Arabidopsis* involves expression of the twin channel subunits KAT1 and KAT2. *J. Biol. Chem.* 276: 3215–3221.

Piñeros, M.A., Cançado, G.M.A. and Kochian, L.V. (2008a) Novel properties of the wheat aluminum tolerance organic acid transporter (TaALMT1) revealed by electrophysiological characterization in *Xenopus* oocytes: functional and structural implications. *Plant Physiol.* 147: 2131–2146.

Piñeros, M.A., Cançado, G.M.A., Maron, L.G., Lyi, S.M., Menassi, M. and Kochian, L.V. (2008b) Not all ALMT1-type transporters mediate aluminum-activated organic acid responses: the case of *ZmALMT1*—an anion-selective transporter. *Plant J.* 53: 352–367.

Preston, G.M., Carroll, T.P., Guggino, W.B. and Agre, P. (1992) Appearance of water channels in *Xenopus* oocytes expressing red cell CHIP28 protein. *Science* 256: 385–387.

Reddy, A.S.N. (2007) Alternative splicing of pre-messenger RNAs in plants in the genomic era. *Annu. Rev. Plant Biol.* 58: 267–94.

Saji, S., Bathula, S., Kubo, A., Tamaoki, M., Kanna, M., Aono, M., et al. (2008) Disruption of a gene encoding C_4-dicarboxylate transporter-like protein increases ozone sensitivity through deregulation of the stomatal response in *Arabidopsis thaliana*. *Plant Cell Physiol.* 49: 2–10.

Sasaki, T., Yamamoto, Y., Ezaki, B., Katsuhara, M., Ahn, S.J., Ryan, P.R., et al. (2004) A wheat gene encoding an aluminum-activated malate transporter. *Plant J.* 37: 645–653.

Schmidt, C., Schelle, I., Liao, Y.-J. and Schroeder, J.I. (1995) Strong regulation of slow anion channels and abscisic acid signaling in guard cells by phosphorylation and dephosphorylation events. *Proc. Natl Acad. Sci. USA* 92: 9535–9539.

Schroeder, J.I. and Keller, B.U. (1992) Two types of anion channel currents in guard cells with distinct voltage regulation. *Proc. Natl Acad. Sci. USA* 89: 5025–5029.

Sutter, J.-U., Sieben, C., Hartel, A., Eisenach, C., Thiel, G. and Blatt, M.R. (2007) Abscisic acid triggers the endocytosis of the *Arabidopsis* KAT1 K^+ channel and its recycling to the plasma membrane. *Curr. Biol.* 17: 1396–1402.

Takano, J., Miwa, K., Yuan, L., von Wirén, N. and Fujiwara, T. (2005) Endocytosis and degradation of BOR1, a boron transporter of

Arabidopsis thaliana, regulated by boron availability. *Proc. Natl Acad. Sci. USA* 102: 12276–12281.

Takano, J., Wada, M., Ludewig, U., Schaaf, G., von Wirén, N. and Fujiwara, T. (2006) The *Arabidopsis* major intrinsic protein NIP5;1 is essential for efficient boron uptake and plant development under boron limitation. *Plant Cell* 18: 1498–1509.

Toyooka, K., Moriyasu, Y., Goto, Y., Takeuchi, M., Fukuda, H. and Matsuoka, K. (2006) Protein aggregates are transported to vacuoles by a macroautophagic mechanism in nutrient-starved plant cells. *Autophagy* 2: 96–106.

Vahisalu, T., Kollist, H., Wang, Y.-F., Nishimura, N., Chan, W.-Y., Valerio, G., et al. (2008) SLAC1 is required for plant guard cell S-type anion channel function in stomatal signaling. *Nature* 452: 483–486.

Ward, J., Mäser, P. and Schroeder, J.I. (2009) Plant ion channels: gene families, physiology, and functional genomics analyses. *Annu. Rev. Physiol.* 71: 59–82.

Weigel, D. and Glazebrook, J. (2002) Arabidopsis: A Laboratory Manual. Cold Spring Harbor Laboratory Press, Cold Spring Harbor, NY.

Yamaguchi, M., Sasaki, T., Sivaguru, M., Yamamoto, Y., Osawa, H., Ahn, S.J., et al. (2005) Evidence for the plasma membrane localization of Al-activated malate transporter (ALMT1). *Plant Cell Physiol.* 46: 812–816.

Zhang, W.-H., Ryan, P.R., Sasaki, T., Yamamoto, Y., Sullivan, W. and Tyerman, S.D. (2008) Characterization of the TaALMT1 protein as an Al^{3+}-activated anion channel in transformed tobacco (*Nicotiana tabacum* L.) cells. *Plant Cell Physiol.* 49: 1316–1330.